

Submitted: July 19, 2024

Revised: August 6, 2024

Accepted: August 27, 2024

The effect of martensite stabilization in titanium nickelide after various methods of pre-deformation: simulation with a single set of constants

A.E. Volkov ¹  , F.S. Belyaev ² , N.A. Volkova ¹ , E.A. Vukolov ¹,M.E. Evard ¹ , T.V. Rebrov ¹¹ St. Petersburg State University, St. Petersburg, Russia² Institute for Problems of Mechanical Engineering RAS, St. Petersburg, Russia a.volkov@spbu.ru

ABSTRACT

Design of shape memory alloy sensors and actuators requires taking into account the martensite stabilization effect, which consists in a shift upward of the reverse martensitic transformation temperatures after preliminary deformation. In this work it is assumed that this effect is due to damage in martensite domain boundaries during pre-straining. This idea is accounted for in a microstructural model by introducing a variable for boundaries damage and formulating evolution equations. The reverse transformation temperature shift is described with one set of constants for three pre-straining modes: deformation of a specimen in the martensitic state, cooling under a constant stress, and deformation in the austenitic state inducing martensite by stress. For Ti50Ni50 and Ti49Ni51 (at. %), the model matches experimental data well for the first two modes and qualitatively for the third.

KEYWORDS

shape memory alloys • titanium-nickel • martensite stabilization • modeling • microstructural model

Acknowledgements. *This work has been supported by the grants the Russian Science Foundation, RSF 23-29-01006.***Citation:** Volkov AE, Belyaev FS, Volkova NA, Vukolov EA, Evard ME, Rebrov TV. The effect of martensite stabilization in titanium nickelide after various methods of pre-deformation: simulation with a single set of constants. *Materials Physics and Mechanics*. 2024;52(4): 91–99.http://dx.doi.org/10.18149/MPM.5242024_9

Introduction

Shape memory alloys (SMA) are widely used in industry and medicine due to their ability to recover the initial shape during the reverse martensitic transformation (MT) at heating after deformation in the low-temperature phase (martensite). For such applications as thermomechanical actuators or thermal sensors it is in many cases important to know at what temperatures will the shape recovery occur.

The characteristic temperatures A_s and A_f , at which the reverse MT in the undeformed material begins and ends, are material constants. However, experiments show that if the material acquired a deformation in the martensitic phase it can retain structure of martensite when heated to temperatures above A_s in the undeformed material. This phenomenon is known as the martensite stabilization effect (MSE). It can be either beneficial or undesirable depending on the application of the SMA. The magnitude of the shift of A_s depends on the degree of prior deformation.

The effect of martensite stabilization in titanium nickelide has been studied since 1991 [1]. It was observed after various pre-deformation treatment (cold rolling, stretching, and shear in the martensitic state, stress-induced MT, cooling under stress from austenite) for mono- and polycrystals of SMA [2–16]. Different hypotheses about the causes of MSE were proposed in [2–16]. S.A. Kustov et al. [11,12] proposed two mechanisms of MSE: one – mechanical stabilization due to pinning martensite boundaries and the second – chemical stabilization due to atomic reordering. In these works mechanical stabilization is related to aging. Thus, time independent MSE is due only to the chemical stabilization. S.P. Belyaev et al. [16] put forward a hypothesis that the main cause of MSE is the damage to intermartensitic boundaries, which hinders the reverse transition and therefore shifts its temperatures upward. This hypothesis was used in [17] for modeling MSE after pre-deformation by stretching in the martensitic state. A new variable ζ , responsible for the degree of intermartensitic boundary damage, was introduced. It was assumed that ζ increases with the degree of martensite orientation. The evolution equations proposed in that work for ζ were used to model MSE caused by pre-deformation of $\text{Ti}_{50}\text{Ni}_{50}$ alloy specimens in the martensitic state up to various values of strain. The obtained dependences for the shift in the onset temperatures of the reverse MT were in good agreement with the experiment. In the present work, the formulae for calculating the evolution of boundaries damage parameter ζ were adjusted and supplemented to model the MSE caused by other methods of pre-straining.

Microstructural model of SMA

Modeling the functional-mechanical properties is an essential and convenient tool for studying phase transformations, phase stability, and thermomechanical behavior of SMAs. The microstructural model described in [17–20] accounts for reversible phase deformation, microplastic deformation (plastic accommodation of martensite), and the evolution of deformation defects. The internal variables of this model are (1) volume fractions of martensite orientation variants obtained by equivalent but differently oriented Bain's deformations; (2) microplastic deformations associated with these variants; (3) densities of oriented and scattered deformation defects. For describing the material structure, a hierarchy of regions is established: a representative volume consists of grains differing in the orientation of crystallographic axes, and each grain contains austenite and martensite variants. Reuss' hypothesis is accepted: the macroscopic strain described by the small strain tensor ε is calculated as the average value of the grain strains ε^{gr} . For crystals, this strain can be divided into the sum of elastic ε^e , thermal ε^T , phase ε^{Ph} , microplastic ε^{mp} , and plastic ε^p components:

$$\varepsilon = \sum_i f_i \varepsilon^{gr}(\omega_i), \quad \varepsilon^{gr} = \varepsilon^e + \varepsilon^T + \varepsilon^{Ph} + \varepsilon^{mp} + \varepsilon^p, \quad (1)$$

where ω_i are the crystallographic orientation axes, f_i are the volume fractions of grains with orientation ω_i , and the sum is taken over all grain orientations (argument ω_i is further omitted). According to the Reuss' hypothesis, the mixture rule is also applied to the phase deformations within each grain:

$$\varepsilon^{gr} = (1 - \Phi_M) \varepsilon^A + \frac{1}{N} \sum_{n=1}^N \Phi_n \varepsilon^{Mn}, \quad \Phi_M = \frac{1}{N} \sum_{n=1}^N \Phi_n, \quad (2)$$

where ε^A and ε^{Mn} are the strains of the austenite and the n -th martensite variant, N is the number of Bain deformation orientation variants, Φ_M is the total volume fraction of martensite in the grain, and Φ_n is the normalized fraction of the n -th martensite variant (so that its volume fraction relative to the grain volume is Φ_n/N). The phase strain of an individual martensite variant is the Bain's deformation D_n that implements the lattice transformation. Since the fraction of the n -th variant is Φ_n/N ,

$$\varepsilon^{Ph} = \frac{1}{N} \sum_{n=1}^N \Phi_n D_n. \quad (3)$$

Microplastic deformations are plastic deformations caused by phase deformation incompatibility. They accommodate martensite and reduce the elastic energy of interphase stresses. A simplified calculation of microplastic deformations is based on the idea that the growth of each Bain martensite variant initiates a combination of shears creating a deformation proportional to the deviator of phase deformation. Thus, we can apply an equation similar to Eq. (3):

$$\varepsilon^{mp} = \frac{1}{N} \sum_{n=1}^N \kappa \varepsilon_n^p dev D_n, \quad (4)$$

where internal variables ε_n^p serve as "measures" of microplastic deformations, $dev D_n$ is the deviator of the tensor D_n , and κ is a material constant. The equations for Φ_n and ε_n^p are formulated in terms of generalized thermodynamic forces – derivatives of the Gibbs potential G with respect to these variables. For a grain,

$$G = (1 - \Phi_M)G^A + \frac{1}{N} \sum_{n=1}^N \Phi_n G^{Mn} + G^{mix}, \quad (5)$$

where G^A and G^{Mn} are eigen potentials of austenite and the n -th martensite variant, without accounting for their interaction, and G^{mix} is the "mixing potential", equal to the elastic energy of interphase stresses. In Eq. (5), the eigen potentials are:

$$G^a = G_0^a - S_0^a(T - T_0) - \frac{c_\sigma^a(T - T_0)^2}{2T_0} - \varepsilon_{ij}^{0T^a}(T)\sigma_{ij} - \frac{1}{2}D_{ijkl}^a\sigma_{ij}\sigma_{kl} \quad (a = A, Mn), \quad (6)$$

where the upper index $a = A$ denotes austenite and $a = Mn$ – n -th martensite variant; G_0^a and S_0^a are Gibbs potential and entropy at the reference stress $\sigma = 0$ and temperature $T=T_0$ (at which $G_0^A = G_0^{Mn}$); $\varepsilon_{ij}^{0T^a}(T)$ are strains of the phases at $\sigma=0$; c_σ^a are specific heat capacities at $\sigma=0$ and D_{ijkl}^a are elastic compliances. For T_0 , the estimate from [21] is accepted: $T_0 = \frac{M_s + A_f}{2}$ (hereinafter M_s , M_f , A_s , A_f are the characteristic transformation temperatures). Calculation of the G^{mix} potential is a very difficult task. As a simplest estimate, a quadratic form is used similar to that in the model developed by E. Patoor et al. [22,23]. It takes into account that this energy increases with an increase in the volume fractions of martensite Φ_n and decreases due to oriented deformation defects b_n , the appearance and movement of which provides plastic accommodation of martensite – plastic deformations ε_n^p :

$$G_n^{mix} = \frac{\mu}{2} \sum_{m,n=1}^N A_{mn}(\Phi_m - b_m)(\Phi_n - b_n), \quad (7)$$

where the matrix (A_{mn}) describes the self-action and interaction of martensite variants. In the TiNi alloy, the primary self-accommodation of martensite is achieved by grouping variants into correspondent variants pairs (CVP) [24–26]. A decrease of G^{mix} energy due to

the formation of CVP is accounted by the proper negative components in the matrix (A_{mn}). The form of this matrix is taken from [17]. From Eqs. (6) and (7) we find the force causing the growth of the n -th variant of martensite:

$$F_n(T, \sigma, \Phi) = -N \frac{\partial G}{\partial \Phi_n} \approx \frac{q_0}{T_0} (T - T_0) + \sigma_{ij} : D_{ij}^n - \mu \sum_{m=1}^N A_{mn} (\Phi_m - b_m). \quad (8)$$

The existence of the hysteresis of the martensite volume fraction dependences on temperature is accounted by introducing a dissipative force F^{fr} , which counteracts the movement of the interface, so that the transformation condition has the form:

$$F_n = \pm F^{\text{fr}}, \quad (9)$$

where the force F_n is determined by Eq. (8), the plus sign corresponds to the direct transformation, and the minus sign – to the reverse. The value of F^{fr} is expressed in terms of the transformation characteristics: $F^{\text{fr}} = q_0(M_s - T_0)/T_0$. The variations laws for the variables b_n and ε_n^p are derived from the condition of microplastic flow:

$$|F_n^p - F_n^\rho| = F^y, \quad (F_n^p - F_n^\rho) dF_n > 0, \quad (10)$$

where F_n^p is the generalized force conjugate to the variables b_n :

$$F_n^p = -N \frac{\partial G}{\partial b_n} = \mu \sum_{m=1}^N A_{mn} (\Phi_m - b_m), \quad (11)$$

F^y and F_n^ρ are forces describing isotropic and kinematic hardening. The microplastic flow condition (10) is similar to the classical plastic flow condition for a uniaxial stress state: generalized forces F_n^p , F^y and F_n^ρ play the role of stress, flow stress and internal (eigen) stress (or back stress), respectively. Microplastic flow generates deformation defects, which in this model are divided into two groups: scattered defects f and oriented defects b_n . The evolution equations for them are proposed in the form:

$$\dot{b}_n = k_b \left(\varepsilon_n^{\text{mp}} - \frac{|b_n|}{\beta^*} \varepsilon_n^{\text{mp}} H(b_n \varepsilon_n^{\text{mp}}) \right), \quad \dot{f} = \sum_{m=1}^N |\dot{\varepsilon}_m^{\text{mp}}|, \quad (12)$$

where k_b , β^* are material constants, H is the Heaviside function. Further we assume that scattered defects create isotropic hardening, and reversible ones – kinematic hardening. This is accounted for by the so-called closing equations – relations between the defect density f and force F^y , as well as between b_n and force F_n^ρ . In this model, they are selected in the simplest form:

$$F^y = a_y f, \quad F_n^\rho = a_\rho b_n, \quad (13)$$

where a_y and a_ρ are material constants. From conditions (9) and (10) and Eqs. (8) and (11)–(13) the evolutionary equations follow, allowing to calculate the increments of the internal variables Φ_n , $\varepsilon_n^{\text{mp}}$, b_n , f_n for given increments of stress and temperature and then using Eqs. (1)–(4) to find the reversible and irreversible macroscopic strains.

Calculation of damage to intermartensitic boundaries

In this paper, the description of the MSE, as well as in [17], is based on the idea of calculating the damage of the intermartensitic boundaries and its effect on the dissipative force F^{fr} . Observations of the structure of the boundaries [16] show that they are damaged during growth of martensitic plates on the late stages of MT, as well as by the growth of some plates at the expense of others during the reorientation of martensite occurring at

the deformation of samples in the martensitic state. Accordingly, in this model, the equations for the evolution of the damaged boundaries are proposed:

$$d\zeta = k_1 \frac{(\Phi_M - \Phi_{crit})H(\Phi_M - \Phi_{crit})}{(1 - \Phi_{crit})(1 + k_3\zeta^2)} d\tilde{r}H(d\tilde{r}), \quad (14)$$

$$d\zeta = \frac{\zeta_1 - \zeta}{\Phi_M(1 + k_3\zeta^2)} d\Phi_M H(d\Phi_M), \quad (15)$$

$$d\zeta = 0, \quad (16)$$

$$\zeta_1 = k_2 \frac{(\Phi_M - \Phi_{crit})H(\Phi_M - \Phi_{crit})}{(1 - \Phi_{crit})} \tilde{r}. \quad (17)$$

Equation (14) is responsible for the change in damage during reorientation of martensite, (15) and (17) – during forward MT, (16) – during reverse MT; k_1 , k_2 , k_3 , Φ_{crit} are the constants of the material, of which k_1 is responsible for the rate of damage growth during reorientation, k_2 – during forward MT, k_3 is responsible for the rate of saturation of the damage; Φ_{crit} is the martensite volume fraction, at which damage growth begins during the direct MT.

The variable $\tilde{r} = r/\Phi_M$, where $r = \frac{1}{2(N-1)} \sum_{n=1}^N |\Phi_n - \Phi_M|$, characterizes the degree of orientation of martensite: $\tilde{r} = 0$ for completely chaotic martensite and $\tilde{r} = 1$ for completely monodomenized martensite. The main hypothesis is that the dissipative force of resistance to the movement of damaged boundaries increases with the increase in their damage. Thus, the dissipative force F^{fr} in the MT condition (9) must be replaced by F_{MSE}^{fr} , which depends on the boundaries damage. In this work, the equation for the force F_{MSE}^{fr} is proposed in the form: $F_{MSE}^{fr} = F^{fr}(1 + \zeta^k)$, where F^{fr} is the force of resistance to the movement of undamaged boundaries, k is the constant of the material, taking into account the nonlinearity of the effect of damage on the friction force and, accordingly, on the shift of the characteristic temperatures of the reverse MT.

Simulation of experiments studying the martensite stabilization effect

For comparison with experimental data, the following calculations were carried out, in which the preliminary strain is produced in three different ways: (1) deformation in the martensitic state due to the reorientation of martensite; (2) cooling under constant stress with accumulation of the strain due to direct MT; (3) deformation in the austenitic state at a temperature, at which martensite is induced by stresses.

The calculated dependences of strain on temperature are shown in Fig. 1. Comparison with the observed shift of the reverse MT start temperature A_s was carried out for $Ti_{50}Ni_{50}$ and $Ti_{49}Ni_{51}$ alloys experimentally studied in [16]. The following values of constants were used. For $Ti_{50}Ni_{50}$ alloy: characteristic temperatures are $M_s = 57$ °C, $M_f = 64$ °C, $A_s = 82$ °C, $A_f = 89$ °C, the latent heat of transformation is $q_0 = -110$ MJ/ m^3 , constants for MSE are $k_1 = 5.6$, $k_2 = 6.0$, $k_3 = 0.75$, $\Phi_{crit} = 0.5$, $k = 1.8$. For $Ti_{49}Ni_{51}$ alloy: characteristic temperatures are $M_s = -20$ °C, $M_f = -33$ °C, $A_s = -7$ °C, $A_f = 3$ °C, the latent heat of transformation is $q_0 = -150$ MJ/ m^3 , constants for MSE are $k_1 = 6.0$, $k_2 = 14.5$, $k_3 = 12.0$, $\Phi_{crit} = 0.5$, $k = 10$.

The temperatures of phase transformations were taken from the study [16], and the other constants were determined on the basis of the data presented in the same work.

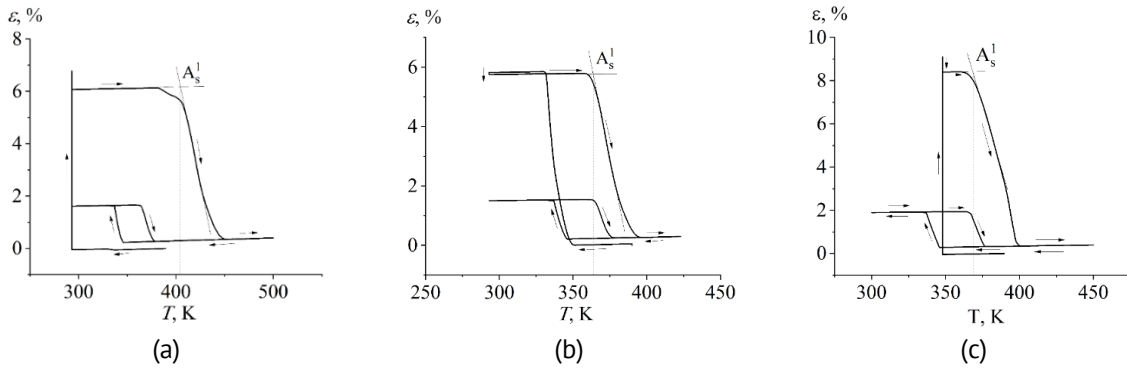


Fig. 1. Dependences of strain on temperature at: preliminary deformation, heating to a completely austenitic state and a subsequent thermal cycle (cooling – heating) showing the effect of the reversible (two-way) shape memory. The preliminary strain is produced by: (a) deformation in the martensitic state; (b) cooling under stress; (c) deformation in the austenitic state producing stress-induced martensite

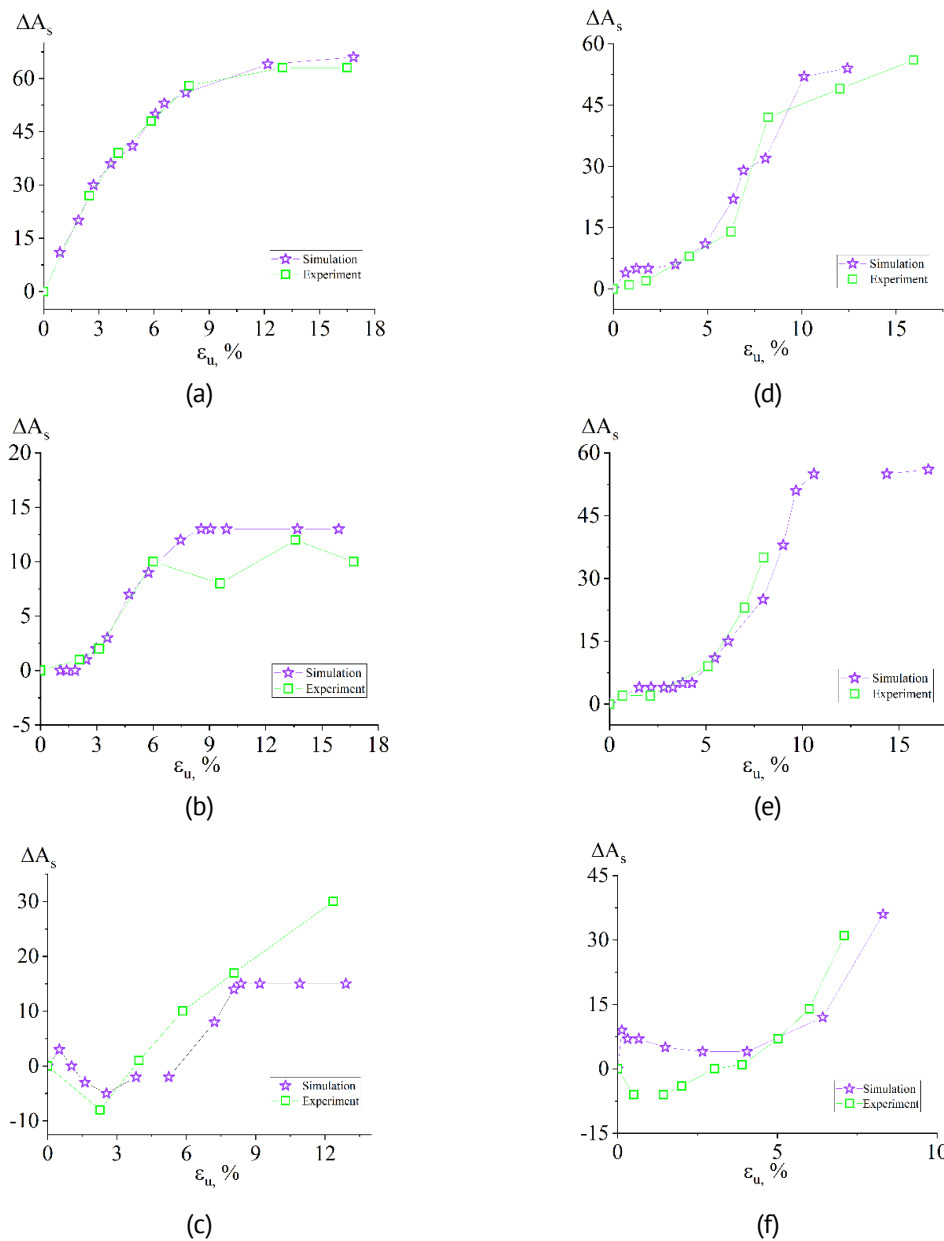


Fig. 2. Dependences of the shift of the reverse MT start temperature $\Delta A_s = A_s^1 - A_s^0$ on the magnitude of the pre-strain for alloys $Ti_{50}Ni_{50}$ ((a) I method, (b) II method, (c) III method) and $Ti_{49}Ni_{51}$ ((d) I method, (e) II method, (f) III method)

Figure 2(a–c) shows the dependences of the shift of the reverse MT start temperature A_s for $\text{Ti}_{50}\text{Ni}_{50}$ alloy on the residual deformation ε_u , produced respectively by the first, second and third methods. The experimental values are taken from [16]. From Fig. 2(a,b) one can see that for the first and second methods of pre-straining, for which the constants were calibrated, the simulation gives results that are in good agreement with the experiment. For the third method of pre-straining (Fig. 2(c)) the calculation also shows good agreement with the experiment, except for large degrees of pre-strain (above 8 %). The results of similar calculations for $\text{Ti}_{49}\text{Ni}_{51}$ alloy are shown in Fig. 2(d–f). It should be noted that the simulation satisfactorily describes the increase in A_s for all three methods of pre-straining, despite the significant difference between the $A_s(\varepsilon_u)$ dependences for $\text{Ti}_{49}\text{Ni}_{51}$ and $\text{Ti}_{50}\text{Ni}_{50}$ alloys. In particular, in the first method of pre-straining for both alloys A_s increases monotonously with ε_u tending to saturation, however, for $\text{Ti}_{50}\text{Ni}_{50}$ alloy the $A_s(\varepsilon_u)$ dependence is convex (Fig. 2(a)), and for $\text{Ti}_{49}\text{Ni}_{51}$ alloy it has a point of inflexion (Fig. 2(d)). The selection of constant values makes it possible to describe the MSE in both of these alloys. A significant discrepancy between the calculated and experimental values of A_s is observed only for $\text{Ti}_{49}\text{Ni}_{51}$ alloy with the third method of pre-straining for low values of ε_u , less than 3 % (Fig. 2(f)).

Conclusion

A hypothesis that the damage of the intermartensitic boundaries during preliminary deformation influences the dissipative force opposing the reverse martensitic transformation can explain the martensite stabilization effect – shift upward of the reverse transformation start temperature A_s . Equations proposed in this paper for calculating the evolution of the boundaries damage make it possible to achieve a satisfactory, and are good description of the martensite stabilization effect appearing after three different methods of pre-straining. Microstructural modeling of the functional and mechanical properties of shape memory alloys $\text{Ti}_{50}\text{Ni}_{50}$ and $\text{Ti}_{49}\text{Ni}_{51}$, performed with an account of the martensite stabilization effect, allow obtaining dependences of the A_s temperature on the magnitude of the preliminary strain. These dependences are in a good quantitative agreement with experimental data in the cases if the pre-strain is produced by deformation of a specimen in the martensitic state or cooling it under a load, and in a good qualitative correspondence in the case of inducing martensite by stress.

References

1. Lin HC, Wu SK, Chou TS, Kao HP. The effects of cold rolling on the martensitic transformation of an equiatomic Ti Ni alloy. *Acta Metallurgica et Materialia*. 1991;39(9): 2069–2080.
2. Piao M, Otsuka K, Miyazaki S, Horikawa H. Mechanisms of the A_s temperature increase by pre-deformation in thermoelastic alloys. *Materials Transactions, JIM*. 1993;34(10): 919–929.
3. Liu Y, Favier D. Stabilisation of martensite due to shear deformation via variant reorientation in polycrystalline NiTi. *Acta Materialia*. 2000;48(13): 3489–3499.
4. Liu Y, McCormick PG. Thermodynamic analysis of the martensitic transformation in NiTi-I. Effect of heat treatment on transformation behaviour. *Acta Metallurgica et Materialia*. 1994;42(7): 2401–2406.
5. Liu Y, Tan GS. Effect of deformation by stress-induced martensitic transformation on the transformation behaviour of NiTi. *Intermetallics*. 2000;8(1): 67–75.

6. Tan GS, Liu Y. Comparative study of deformation-induced martensite stabilization via martensite reorientation and stress-induced martensitic transformation in NiTi. *Intermetallics*. 2004;12(4):373–381.
7. Liu Y. Mechanistic simulation of deformation-induced martensite stabilization. *Materials Science and Engineering: A*. 2004;378(1–2): 459–464.
8. Liu Y, Tan G, Miyazaki S. Deformation-induced martensite stabilisation in [100] single-crystalline Ni–Ti. *Materials Science and Engineering: A*. 2006;438–440: 612–616.
9. Ortin J, Planes A. Thermodynamics of thermoelastic martensitic. *Acta Metallurgica*. 1989;37(5): 1433–1441.
10. Wollants P, Roos JR, Delaey L. Thermally- and stress-induced thermoelastic martensitic transformations in the reference frame of the equilibrium thermodynamics. *Progr Mater Sci*. 1993;37: 227–288.
11. Kustov S, Pons J, Cesari E, Morin M, Van Humbeeck J. Athermal stabilization of Cu–Al–Be $\beta 1'$ martensite due to plastic deformation and heat treatment. *Materials Science and Engineering: A*. 2004;373(1–2): 328–338.
12. Kustov S, Pons J, Cesari E, Van Humbeeck J. Chemical and mechanical stabilization of martensite. *Acta Materialia*. 2004;52(15): 4547–4559.
13. Belyaev S, Resnina N, Iaparova E, Ivanova A, Rakhimov T, Andreev V. Influence of chemical composition of NiTi alloy on the martensite stabilization effect. *Journal of Alloys and Compounds*. 2019;787: 1365–1371.
14. Belyaev S, Resnina N, Rakhimov T, Andreev V. Martensite stabilisation effect in Ni-rich NiTi shape memory alloy with different structure and martensitic transformations. *Sensors and Actuators A: Physical*. 2020;305: 111911.
15. Belyaev S, Resnina N, Ivanova A, et al. Martensite Stabilization Effect in the Ni50Ti50 Alloy After Preliminary Deformation by Cooling Under Constant Stress. *Shape Memory and Superelasticity*. 2020;6: 223–231.
16. Belyaev S, Resnina N, Ponikarova I, Iaparova E, Rakhimov T, Ivanova A. Damage of the martensite interfaces as the mechanism of the martensite stabilization effect in the NiTi shape memory alloys. *Journal of Alloys and Compounds*. 2022;921: 166189.
17. Belyaev FS, Volkov AE, Volkova NA, Vukolov EA, Evard ME, Rebrov TV. Simulation of the effect of martensite stabilization in titanium nickelide after deformation in the martensitic state. *Mechanics of Composite Materials and Structures*. 2023;29(4): 470–482. (In Russian)
18. Belyaev F, Evard M, Volkov A, Volkova N. A microstructural model of SMA with microplastic deformation and defects accumulation: Application to thermocyclic loading. *Materials Today: Proceedings*. 2015;2: S583–S587.
19. Volkov AE, Evard ME, Volkova NA, Vukolov EA. Microstructural modeling of a TiNi beam bending. *Materials Physics Mechanics*. 2023;51(2): 177–186.
20. Belyaev FS, Evard ME, Ostropiko ES, Razov AI, Volkov AE. Aging Effect on the One-Way and Two-Way Shape Memory in TiNi-Based Alloys. *Shape Memory and Superelasticity*. 2019;5(3): 218–229.
21. Salzbrenner RJ, Cohen M. On the thermodynamics of thermoelastic martensitic transformations. *Acta Metallurgica*. 1979;27(5): 739–748.
22. Patoor E, Eberhardt A, Berveiller M. Micromechanical modelling of superelasticity in shape memory alloys. *Le Journal de Physique IV*. 1996;6: C1-277–C1-292.
23. Patoor E, El Amrani M, Eberhardt A, Berveiller M. Determination of the origin for the dissymmetry observed between tensile and compression tests on shape memory alloys. *Le Journal de Physique IV*. 1995;5: C2-495–C2-500.
24. Nishida M, Nishiura T, Kawano H, Imamura T. Self-accommodation of B19' martensite in Ti-Ni shape memory alloys – Part I. Morphological and crystallographic studies of variant selection rule. *Philosophical Magazine*. 2012;92(17): 2215–2233.
25. Madangopal K, Singh J, Banerjee S. Self-accommodation in Ni-Ti shape memory alloys. *Scripta Metallurgica et Materialia*. 1991;25(9): 2153–2158.

About Authors

Aleksandr E. Volkov  

Doctor of Physical and Mathematical Sciences

Professor (St. Petersburg State University, St. Petersburg, Russia)

Fedor S. Belyaev  

Candidate of Physical and Mathematical Sciences

Senior Researcher (Institute for Problems of Mechanical Engineering RAS, St. Petersburg, Russia)

Natalia A. Volkova  

Candidate of Physical and Mathematical Sciences

Associate Professor (St. Petersburg State University, St. Petersburg, Russia)

Egor A. Vukolov  

Student (St. Petersburg State University, St. Petersburg, Russia)

Margarita E. Evard  

Candidate of Physical and Mathematical Sciences

Associate Professor (St. Petersburg State University, St. Petersburg, Russia)

Timofey V. Rebrov

PhD Student (St. Petersburg State University, St. Petersburg, Russia)